

Influence of Molecular Architecture on the Dewetting of Thin Polystyrene Films

R. S. Krishnan and M. E. Mackay*

Department of Chemical Engineering and Materials Science, Michigan State University, East Lansing, Michigan 48824

C. J. Hawker and B. Van Horn

IBM Almaden Research Laboratory, 650 Harry Road, San Jose, California 95210

Received October 20, 2004. In Final Form: April 13, 2005

The control of dewetting for thin polymer films is a technical challenge and of significant academic interest. We have used polystyrene nanoparticles to inhibit dewetting of high molecular weight, linear polystyrene, demonstrating that molecular architecture has a unique effect on surface properties. Neutron reflectivity measurements were used to demonstrate that the nanoparticles were uniformly distributed in the thin (ca. 40 nm) film prior to high temperature annealing, yet after annealing, they were found to separate to the solid substrate, a silanized silicon wafer. Dewetting was eliminated when the nanoparticles separated to form a monolayer or above while below this surface coverage the dewetting dynamics was severely retarded. Blending linear polystyrene of similar molecular weight to the polystyrene nanoparticle with the high molecular weight polystyrene did not eliminate dewetting.

Introduction

Polymer films have numerous technological and biological applications, such as sensors, biomedical devices, insulating dielectric layers, paints, adhesives, etc. Most of these applications require the presence of a continuous and homogeneous film. However, depending on their thickness, polymer films are either metastable or unstable on nonwetable substrates.^{1,2} The rupture and break up of these films is therefore a problem of technological importance, especially for thin films, which are increasingly required in many applications.

The film dewetting rate depends on the surface energy of the substrate, hydrodynamic boundary condition, and film thickness.^{3,4} Much work has been done to understand the dynamics of the dewetting process by considering two primary cases: thick films (>100 nm) that dewet by nucleation and hole growth and thin films (<100 nm) which dewet by spinodal decomposition^{3,5} and/or by film imperfection.^{6,7} Films thinner than the polymer coil size are denoted ultrathin films and they have altogether different dynamics.⁸ Although these studies have helped to further clarify the fundamental mechanism of thin film dewetting, a simple method is still desired to inhibit this undesirable phenomenon.

Various approaches have been adopted to stabilize thin films. Common approaches have been modifying the polymer, such as introducing a specialized end group onto

the polymer with a high affinity for the substrate, or changing the substrate surface energy by irradiation or other mechanisms.^{9–16} Recently, Barnes et al.¹⁷ discovered that fullerene nanoparticles inhibit the dewetting of thin polymer films on silicon substrates. This is contrary to the normal effect of enhanced dewetting by the presence of impurities and other film heterogeneities. Also, Mackay et al.¹⁸ showed that polyether dendrimers¹⁹ can inhibit dewetting of thin polystyrene films. The inhibition of dewetting by the addition of nanoparticles, therefore, seems to be a general phenomenon, however, the underlying physics is still a matter of debate. In this paper, we present the effect of polystyrene nanoparticles and macromolecular architecture²⁰ on the dewetting of polystyrene films. The nanoparticles were made from linear polystyrene macromolecules containing up to ~20% pendent cross-linking groups by an intramolecular collapse strategy where the size and dispersity of the nanoparticle is dictated by the initial linear precursor polymer.

* Corresponding author. Phone: 517-432-4495. Fax: 517-432-1105. E-mail: mackay@egr.msu.edu.

- (1) Reiter, G. *Phys. Rev. Lett.* **1992**, *68*, 75–78.
- (2) Sharma, A.; Reiter, G. *J. Colloid Interface Sci.* **1996**, *178*, 383–399.
- (3) Reiter, G. *Langmuir* **1993**, *9*, 1344–1351.
- (4) Brochardwyart, F.; Degennes, P. G.; Hervert, H.; Redon, C. *Langmuir* **1994**, *10*, 1566–1572.
- (5) Vrij, *Discuss. Faraday Soc.* **1966**, *42*, 23.
- (6) Jacobs, K.; Herminghaus, S.; Mecke, K. R. *Langmuir* **1998**, *14*, 965–969.
- (7) Stange, T. G.; Evans, D. F.; Hendrickson, W. A. *Langmuir* **1997**, *13*, 4459–4465.
- (8) Reiter, G.; de Gennes, P. G. *Eur. Phys. J. E* **2001**, *6*, 25–28.

(9) Kerle, T.; YerushalmiRozen, R.; Klein, J. *Europhys. Lett.* **1997**, *38*, 207–212.

(10) Wunnicke, O.; Muller-Buschbaum, P.; Wolkenhauer, M.; Lorenz-Haas, C.; Cubitt, R.; Leiner, V.; Stamm, M. *Langmuir* **2003**, *19*, 8511–8520.

(11) Yerushalmirozen, R.; Klein, J. *Langmuir* **1995**, *11*, 2806–2814.

(12) Orlicki, J. A.; Moore, J. S.; Sendjarevic, I.; McHugh, A. J. *Langmuir* **2002**, *18*, 9985–9989.

(13) Henn, G.; Bucknall, D. G.; Stamm, M.; Vanhoorne, P.; Jerome, R. *Macromolecules* **1996**, *29*, 4305–4313.

(14) Yuan, C. G.; Meng, O. Y.; Koberstein, J. T. *Macromolecules* **1999**, *32*, 2329–2333.

(15) Yerushalmirozen, R.; Klein, J.; Fetters, L. J. *Science* **1994**, *263*, 793–795.

(16) Feng, Y.; Karim, A.; Weiss, R. A.; Douglas, J. F.; Han, C. C. *Macromolecules* **1998**, *31*, 484–493.

(17) Barnes, K. A.; Karim, A.; Douglas, J. F.; Nakatani, A. I.; Gruell, H.; Amis, E. J. *Macromolecules* **2000**, *33*, 4177–4185.

(18) Mackay, M. E.; Hong, Y.; Jeong, M.; Hong, S.; Russell, T. P.; Hawker, C. J.; Vestberg, R.; Douglas, J. F. *Langmuir* **2002**, *18*, 1877–1882.

(19) Hawker, C. J.; Fréchet, J. M. J. *J. Am. Chem. Soc.* **1990**, *112*, 7638–7647.

(20) Hawker, C. J.; Malmstrom, E. E.; Frank, C. W.; Kampf, J. P. *J. Am. Chem. Soc.* **1997**, *119*, 9903–9904.

Our system is unique in the sense that there are minimum enthalpic interactions between the linear polymer and the nanoparticle and the polymer–nanoparticle interactions would be purely a result of entropic interactions. The nanoparticle used in this study is ca. 4.2 nm in diameter (number average molecular mass (M_n) = 25.3 kDa) and is 20% cross-linked; i.e., every fifth monomer unit of the precursor linear polystyrene chain was cross-linked during the reaction. These nanoparticles have already been shown to dramatically affect the bulk properties of linear polymers.²¹ Mackay et al.²¹ showed that these nanoparticles, when blended with their linear analogues, induce a non-Einstein-like decrease in viscosity. Here, in this work, we find that these nanoparticles also behave similarly to dendrimers and C₆₀ in inhibiting the dewetting of polystyrene films.

Materials and Methods

The syntheses and characterization of polystyrene nanoparticles used in this study are reported elsewhere.²² We use a 25.3 kDa molecular mass nanoparticle where 20% of the monomer units are cross-linked (denoted as tightly cross-linked). Polystyrene standards were obtained from Scientific Polymers (deuterated polystyrene, dPS, M_w = 63.1 kDa, PDI = 1.1; and protonated polystyrene, PS75, M_w = 75.0 kDa, PDI = 1.12; PS19, M_w = 19.3 kDa, PDI = 1.07; M_w is the weight-average molecular mass and PDI is ratio of weight-average to number-average molecular mass; both M_w and PDI were supplied by the manufacturer). The solvent, benzene, was procured from Sigma Aldrich Co.

Both nanoparticle and polystyrene were purified to remove silicon-containing compounds.²³ This was achieved by digesting any silicon-containing contaminants within the nanoparticle/polymer in hydrofluoric acid (HF) for 24 h, the acid does not affect the organic materials. The polymer or nanoparticle was then dissolved in benzene while still in contact with HF. The two solutions were allowed to settle and the organic layer decanted. The solution was then dripped in methanol to precipitate the cleaned polymer/nanoparticle. Separate XPS measurements confirmed that any silicon-containing compounds were removed by the HF treatment. This procedure was found necessary to ensure reproducibility of the results, especially when the melt surface tension was measured.²⁴

Blends were prepared by mixing appropriate volumes of stock solutions (concentration = 5 mg/mL) to obtain solutions containing 1–20% of nanoparticles by weight with respect to the linear polymer. Linear–linear blends were also prepared in the same way as were the blends for the neutron reflectivity experiments. All the solutions were filtered through a 0.2- μ m filter before spin-coating. The silicon wafer substrates were used as received from Wafer World Inc. For dewetting experiments, all the substrates were silanized²⁵ using Sigmacote (Sigma-Aldrich Co.). This was done by spin-coating a thin layer of Sigmacote onto the wafer surface followed by rinsing the surface with water and subsequently spin-coating with the solvent.

The films were prepared by spin-coating, at 5000 rpm for 40 s, from a benzene solution onto freshly cleaved mica sheets²⁶

(21) Mackay, M. E.; Dao, T. T.; Tuteja, A.; Ho, D. L.; Van Horn, B.; Kim, H. C.; Hawker, C. J. *Nat. Mater.* **2003**, *2*, 762–766.

(22) Harth, E.; Van Horn, B.; Lee, V. Y.; Germack, D. S.; Gonzales, C. P.; Miller, R. D.; Hawker, C. J. *J. Am. Chem. Soc.* **2002**, *124*, 8653–8660.

(23) It was essential to remove these silicon-containing compounds such as polydimethylsiloxane (PDMS) and silicone oil that abound in laboratories, as these have lower surface energy and might interfere with the dewetting experiments. For example, surface tension measurements of some of the samples using the micro-Wilhelmy fiber technique showed variable results for samples with and without the silicon-containing compounds.

(24) Dee, G. T.; Sauer, B. B. *J. Colloid Interface Sci.* **1992**, *152*, 85–103.

(25) Muller-Buschbaum, P. *Eur. Phys. J. E* **2003**, *12*, 443–448.

(26) It was not possible to spin coat the benzene solution directly onto the silanized surface, as the contact angle of the solution with the surface was extremely high. Direct spin-coating of the solution resulted in highly nonuniform films.

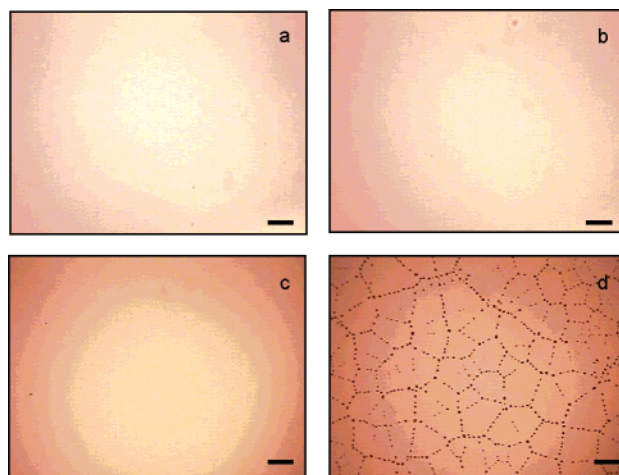


Figure 1. Pure 25.3 kDa nanoparticle film before (a) and after (b) annealing at 160 °C for 24 h. There are no signs of film rupture, even after such extended annealing times. However, the linear polystyrene of comparable molecular mass (19 kDa) dewets in less than 10 min (c and d) on the silanized surface (cf. Figure 3). Film thickness is ca. 40 nm and the length of the scale bar is 100 μ m.

(Ted Pella Inc.). Under these conditions the films produced were approximately 40 nm thick as determined by ellipsometry. They were then floated onto a clean, deionized water surface and picked up by the silanized substrate. The roughnesses of silanized surfaces and the polystyrene films, as determined by atomic force microscopy (Pacific Nanotechnology NanoR AFM), were below 1 nm. The samples for neutron reflectivity measurements were made by direct spin-coating of the polymer solution onto the silanized surface. The surfaces were, however, silanized using Siliclad (Gelest Inc.), which has a higher critical surface energy (γ_c = 32 mJ/m²) which enabled direct spin-coating of the benzene solution. All the films were dried under vacuum for at least 12 h before annealing. This was done to ensure complete removal of the entrapped solvent and other contaminants. The films were mostly annealed in air, but in some cases the annealing was performed under vacuum.

The film morphologies, after annealing, were captured using optical microscopy in the reflection mode. The real-time measurements of the samples were performed by heating them in air under a standard bright field light microscope. The neutron reflectivity measurements were performed at POSY2 Neutron Reflectometer (resolution in q -space, $\Delta q/q$ = 0.05) at Argonne National Laboratory, on polymer blend films that were previously annealed under vacuum at 140 °C for 2 h. The reduced neutron reflectivity data was analyzed using Paratt 32 software from HMI Berlin.

Results and Discussion

Figure 1 shows the optical micrographs of the pure nanoparticle (25.3 kDa) and linear polystyrene (PS19) before and after annealing. Whereas the nanoparticle by itself does not dewet at all, the familiar pattern of Voronoi polygons³ is observed for the dewetting of the equivalent molecular weight linear polymer. This points to the effect molecular architecture has on surface properties. The spreading coefficient S for the wetting/dewetting of a liquid on a solid substrate is defined as

$$S = -\gamma_{LA} + \gamma_{SA} - \gamma_{LS} \quad (1)$$

where γ is the surface energy (tension) for the liquid–air (LA), substrate–air (SA), and liquid–substrate (LS) interfaces. For wetting, $S > 0$, and for dewetting, $S < 0$. The dispersive surface energy of the silanized surface used in this study is ca. 25 mJ/m² at 25 °C, as determined by

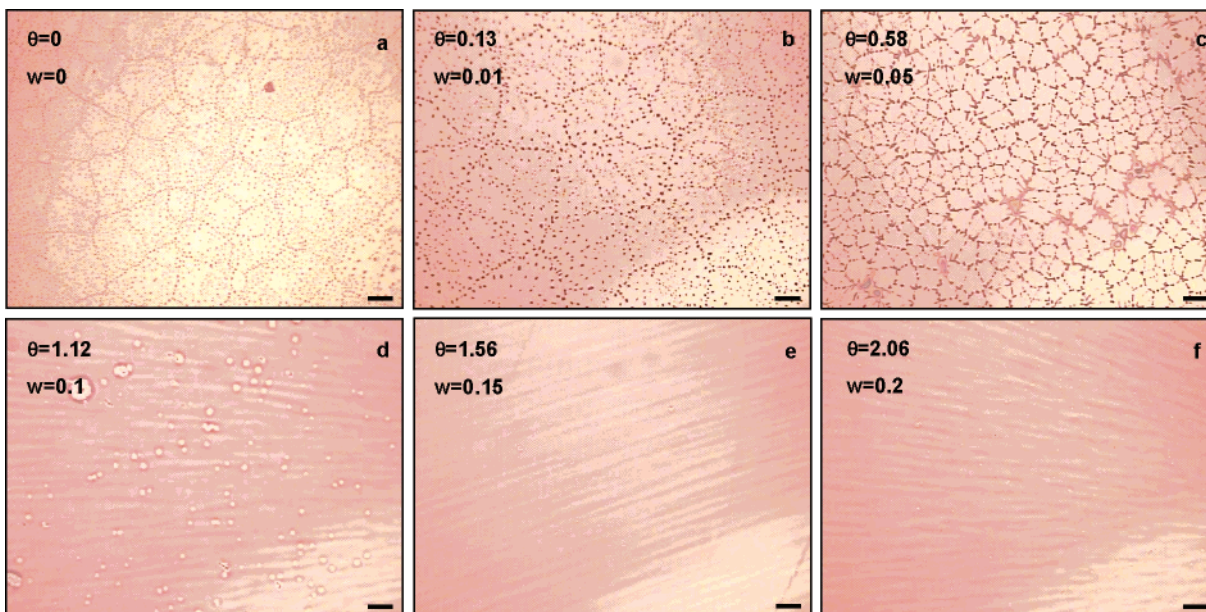


Figure 2. Optical micrographs of blends of 75 kDa linear polystyrene with 25.3 kDa nanoparticle. All the films were annealed for >24 h in a vacuum: (a) Pure PS, (b) 1%, (c) 5%, (d) 10%, (e) 15%, and (f) 20% nanoparticle concentration. Note, at 0.15–0.20 nanoparticle weight fraction (w), the dewetting is completely eliminated (aerial fraction, $\theta \sim 1.5$ –2.0). Film thicknesses are ca. 40 nm, and the length of the scale bars is 100 μm .

the Fowkes method.²⁷ The surface tension²⁴ of PS19 at 160 °C is approximately 27 mJ/m². Assuming that the polystyrene chains only interact with the substrate through dispersive forces, it can be concluded that the dewetting of the linear polymer occurs at that temperature because the surface tension of the polymer is higher than the surface energy of the substrate, causing the spreading coefficient, S , to be negative.

The fact that the nanoparticle by itself does not dewet has an important implication. By simply changing the molecular architecture of the polymer it is possible to tune its surface properties. We have tried to measure the surface tension of the nanoparticle at high temperatures, but the data does not suggest wetting, as anomalously high forces were measured with the Wilhelmy microfiber technique²⁸ and a melt surface tension on the order of 150 mN/m is recorded at 240 °C. This suggests an alternative explanation for the unusual wetting by the nanoparticle at temperatures much higher than its glass transition ($T_g = 97$ °C). For example, a yield stress could stabilize the film, yet rheological measurement indicates a terminal viscosity for the bulk sample of this nanoparticle.²¹ We believe that contemporary rheological characterization (Rheometrics ARES rheometer) of the nanoparticle system destroys the structure, and the microfiber technique is quite sensitive to this type of flow property.

To better understand the surface properties of these cross-linked nanoparticles, we blended them with linear polystyrene of higher molecular weight ($M_w = 75$ kDa). Previously, Barnes et al.¹⁷ and Mackay et al.¹⁸ found that fullerenes and dendrimers inhibit or delay the dewetting of linear polystyrene. In both cases, it was speculated that the nanoparticles separate to the substrate and form a diffuse layer, which in turn pinned the contact lines of the growing holes, thereby arresting dewetting, or change the surface energy by creating a fractal-like nanoroughness. In some cases, use of higher concentrations of these

nanoparticles completely eliminated dewetting. In both of these studies the molecular weight of the polystyrene used was on the order of 15 kDa, which has a low viscosity and dewets very quickly, depending on the surface energy of the substrate.²⁵ In this work we silanized our substrates to ensure the reproducibility of the results,²⁹ enabling us to quantify the effect of nanoparticle-induced stabilization of thin films on this low-energy surface.

We blended the 25.3 kDa nanoparticle, concentration ranging from 1 to 20 wt %, with PS75, and Figure 2 shows the optical micrographs of these blend films after annealing. The thickness of these films was ca. 40 nm as determined by ellipsometry and were annealed for more than 24 h at 160 °C under vacuum. Clearly at around 15–20% weight fraction, the dewetting is completely eliminated. To rule out any molecular weight effects, we blended PS19 with PS75 in the same concentration range as above. The goal of this study was to serve as a control for the dewetting kinetics of the nanoparticle–linear polymer blends. All the linear–linear polymer blend films dewetted, yet some discussion on these systems is warranted prior to discussion of the nanoparticle–linear polymer blends.

Figure 3 shows the rate of hole growth of the blends with time, demonstrating that increasing the PS19 concentration in PS75 actually *decreases* the rate of hole growth, which is counterintuitive, as one would expect the dewetting rate to be faster since the blend has a lower viscosity than the pure polymer (PS75). The viscosity varies as $M_w^{3.4}$, so the viscosity of the blend will be lower than that of the pure polymer. For example, for the 10 wt

(27) Fowkes, F. M.; McCarthy, D. C.; Mostafa, M. A. *J. Colloid Interface Sci.* **1980**, *78*, 200–206.

(28) Sauer, B. B.; Dipalo, N. V. *J. Colloid Interface Sci.* **1991**, *144*, 527–537.

(29) Acid cleaning of the silicon wafers results in highly hydrophilic substrates. Air-borne hydrocarbons deposit on these high-energy clean surfaces, creating a thin layer of contamination. The presence of this layer is very important for dewetting/wetting. The uncontrollable thickness and the nonuniform nature of this contamination layer resulted in highly inconsistent wetting/dewetting behavior of the polymer. To ensure the dewetting of the pure polymer and to be able to reproduce the same surface again, it was essential to silanize our substrates. This resulted in a substrate of very low and uniform surface energy.

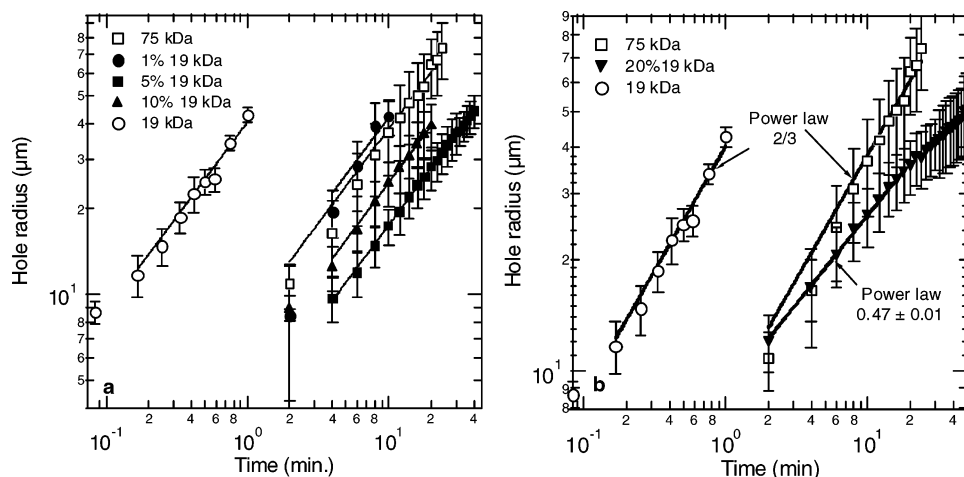


Figure 3. (a) Hole radius versus time during aging at 160 °C for pure linear PS75, PS19, and their blends along with power law fits. All the systems have been modeled with a power law model, and the growth exponent was fixed at 2/3 (represented by the solid lines). Each data point is an average of ca. 30 holes over three samples. The power law prefactor, A , is given in Table 1. (b) A 20% PS19 blend behaves fundamentally different and an initial power law of ~ 0.5 is seen; however, this value is not constant. All films are ca. 40 nm thick.

Table 1. Values of the Prefactor, A , As Determined for the Linear–Linear Blends of Polystyrene Shown in Figure 3^a

% PS19	prefactor A ($\mu\text{m}/\text{s}^n$)	% PS19	prefactor A ($\mu\text{m}/\text{s}^n$)
0	8.2	10	5.3
1	8.8	20 ^a	4.1
5	3.7	100	40.4

^a Note that for pure PS19 the value of A is 5 times greater than that for pure PS75. However, addition of the low molecular weight polymer actually reduces the value of A with respect to the higher molecular weight polymer. The value of A for the 20% blend is based on $n = 0.4$; all other cases have $n = 2/3$.

% blend, the reduction in viscosity is almost 7%^{30,31} with respect to the pure higher molecular weight linear polymer.

A theoretical description of the dynamics of hole growth has been developed in previous studies.^{4,32,33} In general, the hole radius (R) in a polymer film grows with time (t) as $R \sim t^n$, where n is the hole growth parameter whose value depends on the hydrodynamic boundary condition at the polymer substrate interface. In these studies the rate of hole growth was divided into two regimes: if the polymer was allowed to slip on the substrate, the hole radius grows with time as $R \sim t^{2/3}$ ($n = 2/3$). If instead there is no slip, then the radius scales as $R \sim t$ ($n = 1$). The polymer is expected to slip on an extremely smooth surface or an “ideal” surface.³³ A silanized surface is close to an ideal surface, albeit chemically dissimilar, as it is a thin, smooth compact molecular surface of aliphatic chains.

As shown in Figure 3, the rate of dewetting slows with increasing concentration of the lower molecular weight polymer. Table 1 lists the values of the prefactor A for each of the blends and should be inversely proportional to the viscosity. Even though there is a substantial decrease in viscosity, the apparent decrease in the value of A suggests otherwise. It is also interesting to note that the 20 wt % blend does not follow the usual growth trend

as the rest of the blends. The growth exponent (n) for this blend was found to be ~ 0.5 , unlike 2/3 for other blends. This is clearly shown in Figure 3 when compared to results for pure PS19 and PS75. So the dewetting behavior for this blend is outside the perfect slipping regime.^{34,35}

The work by Hariharan et al.³⁶ and Schaub et al.³⁷ suggest that there is an entropy driven segregation of the lower molecular weight polymer to the substrate. The migration of the lower molecular weight polymer to the substrate may alter the spreading coefficient by changing the surface roughness and/or energy at the interface. Should the lower molecular weight polymer (PS19) separate to the substrate, the fractional aerial coverage (θ) can be estimated through a simple mass balance as

$$\theta = (\Delta/2R_g)\phi \quad (2)$$

where Δ is the film thickness, R_g , the radius of gyration of the separating polymer, and ϕ , the bulk polymer volume fraction. The radius of gyration (R_g) of linear polystyrene is given by³⁸

$$R_g \text{ (nm)} = 0.87 \times [M_w \text{ (kDa)}]^{0.5} \quad (3)$$

Therefore, for PS19, $R_g = 3.8$ nm, and a 20% blend in a 40 nm thick film has a fractional coverage (θ) of 1.05. This means that at 0.2 volume fraction there is a monolayer of the lower molecular weight polymer at the solid substrate. Of course, at smaller concentrations of the low molecular weight polymer, the fractional coverage is submonolayer.

To understand how this migration affects the dewetting kinetics, we review the considerable amount of work done on the wetting behavior of polymer melts on brushes of identical molecules (autophobicity).^{11,13,39,40} It has been determined that the polymer brush density is an important

(30) Onogi, S. H. K.; Ueki, S.; Ibaragi, T. *J. Polym. Sci.: Part C* **1966**, *15*, 481–494.

(31) Masuda, T. K. K.; Inoue, T.; Onogi, S. *Macromolecules* **1969**, *3*, 116–125.

(32) Redon, C.; Brzoska, J. B.; Brochardwyart, F. *Macromolecules* **1994**, *27*, 468–471.

(33) de Gennes, P. G. *C. R. Acad. Sci. Paris Ser. B* **1979**, 219.

(34) Jacobs, K.; Seemann, R.; Schatz, G.; Herminghaus, S. *Langmuir* **1998**, *14*, 4961–4963.

(35) Neto, C.; Jacobs, K. *Physica A* **2004**, *339*, 66–71.

(36) Hariharan, A.; Kumar, S. K.; Russell, T. P. *Macromolecules* **1990**, *23*, 3584–3592.

(37) Schaub, T. F.; Kellogg, G. J.; Mayes, A. M.; Kulasekera, R.; Ankner, J. F.; Kaiser, H. *Macromolecules* **1996**, *29*, 3982–3990.

(38) Cotton, J. P.; Decker, D.; Benoit, H.; Farnoux, B.; Higgins, J.; Jannink, G.; Ober, R.; Picot, C.; Cloizeau, J. *Macromolecules* **1974**, *7*, 863–872.

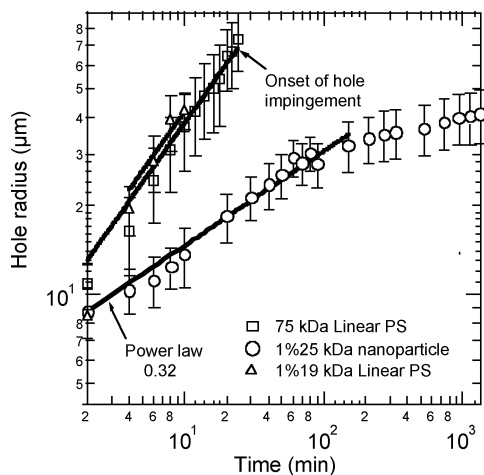


Figure 4. Hole growth as a function of time for pure 75 kDa linear polymer and its 1% blend with 19 kDa linear polystyrene and 25.3 kDa tightly cross-linked nanoparticle at 160 °C. Clearly with just 1 wt % ($\theta = 0.13$) addition of the nanoparticle, the rate of dewetting has drastically slowed, emphasizing the effect of molecular architecture on dewetting. Also note that the growth exponent for the 1% blend is initially 0.32. All films are ca. 40 nm thick.

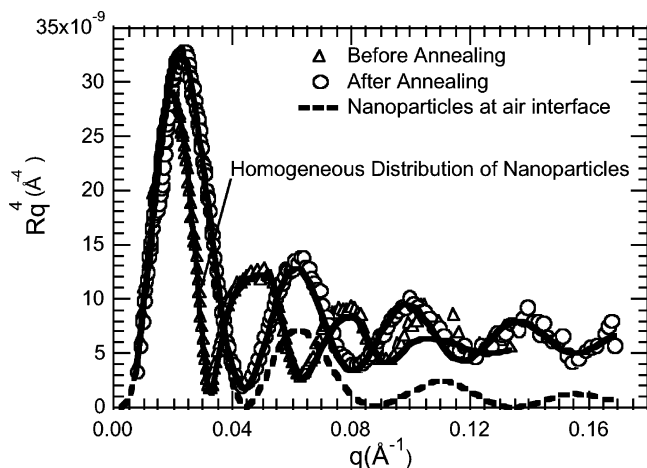


Figure 5. Reflectivity multiplied by reflectance wave vector to the fourth power (Rq^4) vs q for a silanized silicon wafer spin-coated with 63 kDa deuterated polystyrene blended with 10 wt % 25.3 kDa protonated, tightly cross-linked polystyrene nanoparticles before and after annealing at 140 °C for 2 h under vacuum. The dotted line represents the reflectivity profile fit if the nanoparticles separated to the air interface. The solid lines represent the fits for the films before and after annealing as described in the text.

parameter and that slipping of a polymer melt on top of brushes of identical molecules depends on the interaction between the film and the brush,^{41–43} with a weaker interaction implying stronger slippage. Liu et al.⁴⁴ suggest that an energy penalty in stretching a brush affects the wetting properties, and when the ratio of the polymer to brush molecular weight is in excess of ~ 5 , then dewetting will occur.

Table 2. Parameters Used in Parratt32 Software (from HMI Berlin) to Fit the Data in Figure 5^a

system treatment	layer	thickness (Å)	SLD (10^6 Å^{-2})	roughness (Å)
before annealing	1	169	5.80	1
	wafer	–	2.07	15
after annealing	1	142	6.42	1
	2	21	4.59	21
	wafer	–	2.07	11

^a An air interface is assumed at the top of the first layer. The roughness of layer 2 used in the simulation of the film after annealing is extreme and represents an empiricism to generate a scattering length density profile. Other modeling with many layers near the wafer surface generates a similar scattering length density (SLD) profile. The system consisted of 10 wt % 25.3 kDa protonated polystyrene nanoparticles blended with 63 kDa deuterated linear polystyrene and was annealed at 140 °C for 2 h.

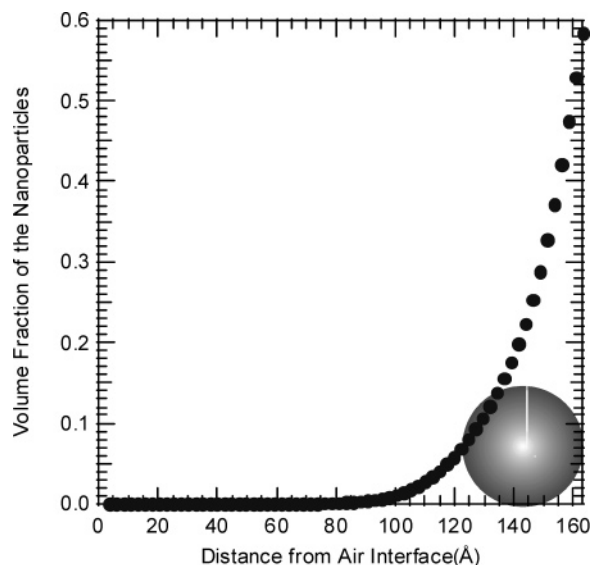


Figure 6. Nanoparticle concentration profile determined from the parameters listed in Table 2 for the film after annealing. A scaled representation of the nanoparticle is placed in the lower right hand corner.

Our system is clearly different from a polymer brush; low molecular weight polymer (probably) separates to the solid substrate, and both components slip along it. Note the molecular weight ratio is ~ 4 and dewetting may be predicted. Yet, when the separated polymer approaches a monolayer, drastic changes in the dewetting kinetics appear, and so an exact parallel between autophobic dewetting from a brush and our system cannot probably be made. Conjecture to a probable mechanism is not given here; it is important to note that at all low molecular weight linear polymer concentrations dewetting is present and a change in the dewetting kinetics is apparent when a monolayer is present.

As shown in Figure 2, either the blends of nanoparticle–linear polymer do not dewet or there is a marked reduction in the dewetting velocity. This is graphically illustrated in Figure 4, where the rate of hole growth for pure PS75 (25.3 kDa) and also with the low molecular weight linear polymer (PS19) at the same concentration. As discussed above for the 20% linear–linear blend, the 1% nanoparticle blend does not show perfect slippage, or a complicated dewetting mechanism is present. The rate of dewetting has drastically slowed even at 1% nanoparticle addition. Indeed, Mackay et al.²¹ found that addition of 1% of the nanoparticle caused a substantial decrease in the viscosity, of course, implying a faster rate of dewetting.

(39) Reiter, G.; Auroy, P.; Auvray, L. *Macromolecules* **1996**, *29*, 2150–2157.

(40) Gay, C. *Macromolecules* **1997**, *30*, 5939–5943.

(41) BrochardWyart, F.; Gay, C.; deGennes, P. G. *Macromolecules* **1996**, *29*, 377–382.

(42) Durliat, E.; Hervet, H.; Leger, L. *Europhys. Lett.* **1997**, *38*, 383–388.

(43) Reiter, G.; Khanna, R. *Phys. Rev. Lett.* **2000**, *85*, 2753–2756.

(44) Liu, Y.; Rafailovich, M. H.; Sokolov, J.; Schwarz, S. A.; Zhong, X.; Eisenberg, A.; Kramer, E. J.; Sauer, B. B.; Satija, S. *Phys. Rev. Lett.* **1994**, *73*, 440–443.

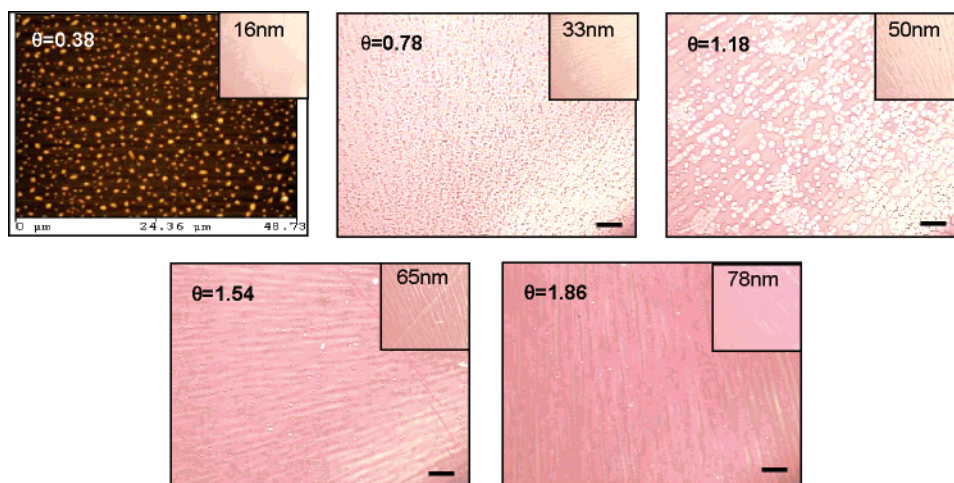


Figure 7. Optical micrographs of 10 wt % blends of 75 kDa linear polystyrene with 25.3 kDa polystyrene nanoparticles (tightly cross-linked) at various surface coverage. The surface coverage (θ) was varied by changing the film thickness from 16, 33, 50, 65, and 78 nm, as indicated in the micrographs. All the films were annealed for >24 h in air at 170 °C, and when $\theta > 1.5$, the dewetting is almost eliminated. The insets show the film before annealing. The length of the scale bar is 100 μm . Note that for the 16 nm film, an atomic force micrograph has been shown for the film after annealing due to difficulties utilizing optical microscopy with this sample. In this case, the image size is approximately 50 $\mu\text{m} \times 50$ μm . Also note that for films thicker than 50 nm, some complicated surface features (buckling instabilities) are present in films both before and after annealing, due to the spin-coating process.

Since bulk transport properties do not appear to explain our results, surface effects could certainly explain this observation as postulated in the control experiments performed with the linear 19.3 kDa polymer. We performed neutron reflectivity measurements on a 10 wt % representative sample before and after annealing. The film was ca. 17 nm thick and was annealed under vacuum for 2 h at 140 °C prior to the measurement. Figure 5 shows the neutron reflectivity data for a 10 wt % blend of 25.3 kDa protonated nanoparticle blended with 63 kDa deuterated linear polystyrene film (R is the reflectivity). The fitting parameters used for the data are shown in Table 2 and the film before annealing was modeled as a single layer with a homogeneous distribution of nanoparticles. The film after annealing was modeled in many ways, including a gradual gradient profile, nanoparticles at the air-polymer interface (dashed line in Figure 5), and nanoparticles at the polymer-wafer interface. Only the latter model predicted the reflectivity profile correctly.

To rule out migration of the nanoparticles due to any deuteration effects,⁴⁵ we did neutron reflectivity on similar films (data not shown) with different deuteration contrast (i.e., partially deuterated nanoparticles in protonated linear polymer and partially deuterated nanoparticles in deuterated linear polymer). Changing the deuteration did not affect the migration of the nanoparticles to the solid substrate. Also, since both the nanoparticle and the linear polymer have identical repeat units (styrene monomer), the enthalpic interactions between the nanoparticles and the linear polymer is minimal³⁶ and the migration of the nanoparticles to the solid substrate is primarily an entropic effect.

When fitting aged nanoparticle films' data, the roughness at the nanoparticle-wafer interface was extremely large (cf. Table 2). However, this is an empiricism of the model and the roughness has no physical meaning; equivalent fits were found upon assuming multiple layers with an equivalent scattering length density profile. The scattering length density profile generated from this model changed more gradually than that for a sharp interface,

yet the plateau for Rq^4 vs q is a signature for a fairly sharp interface. As seen in Figure 5, it seems that the nanoparticles migrate to the solid substrate surface, since other scattering length density profiles do not fit the data at all.

One can convert this profile to a concentration and this was done as shown in Figure 6 with a scaled representation of the nanoparticle in the lower right hand corner of the graph. It is clear that the concentration profile changes substantially near the substrate surface and that the concentration profile correlates almost exactly with the nanoparticle size. On the basis of experiments with other deuteration levels (i.e. partially deuterated nanoparticle in either protonated or deuterated polystyrene) and substantial modeling, we believe that the polystyrene nanoparticles separate to the substrate surface, forming a reasonably coherent layer. Note, according to eq 1, the nanoparticle areal coverage for this sample should be ~ 0.4 , so a coherent layer is not present at the substrate. Instead, a layer of protonated nanoparticles mixed with deuterated linear polymer is at the substrate.

To ascertain a possible mechanism for this observation, the nanoparticle fractional coverage at which the dewetting is completely eliminated in Figure 2 was determined. According to eq 1, taking the particle diameter (really $2R_g$) to be 4.2 nm, which we have determined separately through small angle neutron scattering, we find dewetting is eliminated when a fractional coverage on the order of 1–1.5 is present.

To clarify if the areal coverage is the determining factor, a final series of experiments was performed. Changing the film thickness while the bulk concentration is kept constant is equivalent to varying the bulk concentration while the thickness is kept constant; see eq 1. This was done by keeping the bulk concentration at 10% and changing the film thickness from 16 to 78 nm, with results shown in Figure 7. All films were annealed for time greater than 24 h at 170 °C in air. Again it is found that an areal coverage of 1–1.5 is necessary to eliminate dewetting, in agreement with Figure 2.

The physics of the separated layer will clearly be different from those for a brush layer, and whether arguments given by others^{43,44} can be used with our system

(45) Jones, R. A. L.; Kramer, E. J.; Rafailovich, M. H.; Sokolov, J.; Schwarz, S. A. *Phys. Rev. Lett.* **1989**, *62*, 280–283.

is unclear. For example, nanoroughness affects surface wetting behavior,⁴⁶ so a nanoparticle rich layer may alter the spreading coefficient by changing the roughness of that interface. Further, recent simulations⁴⁷ show that the mechanism of dewetting inhibition is affected by nanoparticle mobility on a substrate, the interaction between the nanoparticle and the polymer, and also the size of the nanoparticle. These simulations were based on the work of Barnes et al.,¹⁷ where the ratio of the size of the nanoparticle to that of the polymer R_g was on the order of 0.4. According to ref 46, a weak interaction between the polymer and the nanofillers would tend to agglomerate the nanoparticles and enhance the dewetting. In our system, the enthalpic interaction between the nanoparticle and the polymer is almost negligible, yet dewetting can be eliminated.

Finally, even though the nanoparticles separate to the solid substrate, the mechanism for dewetting inhibition may be different than that for fullerenes. According to the Douglas hypothesis,^{17,48} the nanoparticles separate to the solid substrate and create fractal-like trees that pin contact lines and modify the conformational energy of the linear polymer. This hypothesis may not apply to our system, due to the nanoparticle size and layer thickness exemplified in Figure 6. An alternate hypothesis is that the separated layer merely changes the global surface energy

(46) Ramos, S. M. M.; Charlaix, E.; Benyagoub, A.; Toulemonde, M. *Phys. Rev. E* **2003**, *67*, 031604–031601/031604–031606.

(47) Luo, H.; Gersappe, D. *Macromolecules* **2004**, *37*, 5792.

(48) Barnes, K. A.; Douglas, J. F.; Liu, D. W.; Karim, A. *Adv. Colloid Interface Sci.* **2001**, *94*, 83–104.

equivalent to silanizing, yet with polystyrene nanoparticles. Why this is more effective with a nanoparticle architecture than a linear polymer is not clear and may be related to the associated dynamics along the substrate surface.

Conclusion

It has been shown that addition of polystyrene nanoparticles to thin polystyrene films inhibits and in some cases eliminates dewetting, as long as an enriched layer of nanoparticles is present at the substrate surface. Since the nanoparticles are compositionally very similar to the bulk linear polymer, it is apparent that molecular architecture plays an important role in eliminating dewetting. Addition of low molecular weight, linear polymer to longer, linear chains does not eliminate dewetting, but the dewetting rate is slower. It is clear that the separated component's dynamics along the substrate is important to influence the dewetting kinetics and promote wetting.

Acknowledgment. Funding from Michigan State University, Argonne National Laboratory, and NSF-NIRT 0210247 is greatly appreciated. Conversations with Dr. Bryan Sauer, DuPont Central Research and Development, were very helpful, particularly regarding the influence of a yield stress on surface tension measurements. We appreciate time at the Argonne National Laboratory given to us to perform reflectivity measurements.

LA0474060